A Fully Integrated, Ready-to-Use Distance-Based Chemosensor for Visual Quantification of Multiple Heavy Metal Ions

Wang, Gaobo; Li, Jiaheng; Wu, Siying; Jiang, Tianyi; Chen, Ting-Hsuan

Published in:
Analytical Chemistry

Published: 22/11/2022

Document Version:
Post-print, also known as Accepted Author Manuscript, Peer-reviewed or Author Final version

Published version (DOI):
10.1021/acs.analchem.2c04712

Publication details:
Wang, G., Li, J., Wu, S., Jiang, T., & Chen, T.-H. (2022). A Fully Integrated, Ready-to-Use Distance-Based Chemosensor for Visual Quantification of Multiple Heavy Metal Ions. *Analytical Chemistry*, *94*(46), 15925–15929. https://doi.org/10.1021/acs.analchem.2c04712

A fully integrated, ready-to-use distance-based chemosensor for visual quantification of multiple heavy metal ions

Gaobo Wang[a]†, Jiaheng Li[a]†, Siying Wu[a], Tianyi Jiang[b] and Ting-Hsuan Chen[a]*

[a]Department of Biomedical Engineering, City University of Hong Kong, Hong Kong Special Administrative Region, 999077, China

[b]School of Mechatronics Engineering, Harbin Institute of Technology, 150001, Harbin, Heilongjiang Province, China

*Email: thchen@cityu.edu.hk

Point-of-care devices offering quantitative results with simple steps would allow great useability for untrained end-users. Here, we report a ready-to-use chemosensor integrating automatic sample metering, on-chip reaction, gravitational-magnetic separation, and a distance-based readout for visual quantification of multiple heavy metal ions. Deoxyribozymes (DNAzymes), probe-modified magnetic microparticles (MMPs) and polystyrene microparticles (PMPs) were preloaded into a microfluidic chip and freeze-dried. After collecting the water sample with automatic sample metering, the particles were resuspended, and the MMPs and PMPs hybridized with DNAzyme at its two termini, forming the "MMPs-DNAzyme-PMPs" structure. When target metal ions were present, the DNAzymes were cleaved, yielding an increased number of free PMPs. All on-chip reactions were controlled by stopping the liquid flow using capillary valves and bursting it with hand-controlled tilting. Using the chip with a gravitational-magnetic separator, the free PMPs were separated from "MMPs-DNAzyme-PMPs" due to gravity and accumulated into the trapping channel with a nozzle, forming a visual bar with growing distances proportional to the concentration of target metal ions. The achieved limit of detection (LOD) for Cu^{2+} (103.1 nM), Pb^{2+} (69.5 nM), and Ag^{+} (793.6 nM) are below the maximum contamination levels. High selectivity of 100-fold, 200-fold, and 20-fold against interferences was obtained. Moreover, by integrating three identical channels in parallel, simultaneous detection of the above-mentioned heavy metal ions in fresh and tap water samples was also investigated with high accuracy. Together, this fully integrated and easy-operated platform embodies excellent potential as rapid, on-site sensing for unskilled users.

Heavy metal ions are harmful not only to the ecological environment but to human health.[1,2] With high toxicity and low biodegradability, they are prone to be enriched in the food chain and cause irreversible physiological consequences for human beings. In this regard, rapid, sensitive, and decentralized routine inspection is urgently needed. Although portable electrochemistry-based platforms with fast response and high sensitivity have been developed, they typically need complicated fabrication processes and are fragile to co-exist interfering factors in the water samples.[3] On the other hand, lateral flow assays (LFAs) are portable and affordable but only provide qualitative or semi-quantitative measurements.[4,5] Despite the efforts dedicated to enhancing the performance of lateral flow assays by combining with digital devices for quantitative measurement,[6,7] the requirement for additional appliances goes against the original intention of portable and on-site testing.

As such, a point-of-care device that directly displays quantitative measurement without relying on any additional device is highly preferred. Among the approaches displaying quantitative results, the distance-based readout with a thermometer-like appearance has been shown more advantageous than fluorescence and electrochemical signals since it enables the direct visualization of quantitative results owing to the decentralization.[8] While paper analytical devices with distance-based motifs have been developed,[9,10] the analytical performance significantly relies on the accurate loading sample volume in order to obtain consistent results, which requires precise micro pipetting skills, making it unsuitable for non-expert users. Moreover, the generation of distance-based signals in paper analytical devices was essentially a colorimetric strategy that may result in low accuracies of assays due to obscure displaying.[11] Alternatively, the distance-based readout can be attained by means of the formed visual ink bar generated from the production of O_2 from catalyzed H_2O_2.[12] However, perfect sealing during device operation is needed and error-prone. In contrast, we have recently reported a portable microfluidic chip using the accumulated polystyrene microparticles (PMPs) at a microfluidic dam to provide a more reliable and accurate distance displaying. The magnetic microparticles (MMPs) and PMPs were designed to connect with a metal-sensitive DNAzyme, forming "MMPs-DNAzyme-PMPs" structure. With the presence of target metal ion, the DNAzyme is cleaved, resulting in an increasing number of free PMPs, which can be trapped in the

trapping channel, forming a visual bar with the trapping distances proportional to the concentration of target metal ion.[13-15] However, concern arises because the substances used for reactions needs to be freshly prepared with precise pipetting, mixing, and washing before conducting each assay, which is still impractical for the general public who lack professional training and again makes the platform far away from "ready-to-use". So far, a point-of-care platform that minimizes preparation steps and offers quantitative results is yet achieved.

To address those limitations, we report a fully integrated platform consisting of three chambers in a macro-scale (1 mm in height) for automatic sample metering, reaction, and separation. A micro-scale trapping channel (25 μm in height) is used to trap and accumulate free PMPs to form the visual bar (Figure 1A). The device consists of a PDMS and a NOA63 layer fabricated using 3D printing and soft lithography, respectively (Figure S1). The DNAzyme was designed to connect MMPs and PMPs such that the "MMPs-DNAzyme-PMPs" sandwich structure was formed when target metal ions were absent. With the presence of target metal ions, the DNAzyme was cleaved, resulting in disconnection between MMPs and PMPs (Figure 1B).

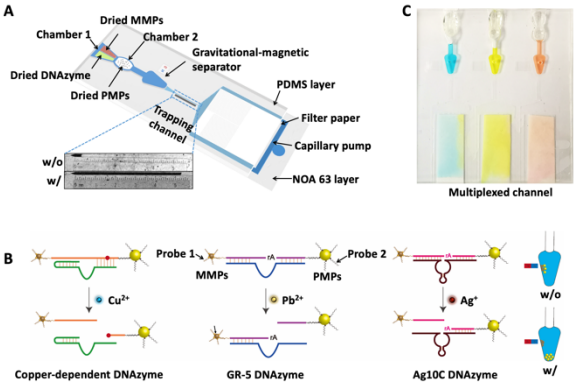

Figure 1. (A) Schematic illustration of the chip with preloaded substances. (B) Cleavages of copper-dependent, lead-dependent (GR-5), and silver-dependent (Ag10C) DNAzyme and their connections with MMPs and PMPs. (C) Demonstration of an integrated device for simultaneous loading and reaction with different food dye dried in chambers.

The water sample was first introduced into chamber 1 with metered volume and to resuspend the DNAzyme and MMPs (0.3 μm in diameter) which were preloaded and freeze-dried. After DNAzymes cleavage and connection with MMPs (Video S1 and Video S2), the device was tilted, allowing the solution to enter chamber 2 to resuspend and react with dried PMPs (15.3 μm in diameter). Afterward, the platform will be placed vertically to allow the reacted substances to flow into a gravitational-magnetic separator where MMPs and "MMPs-DNAzyme-PMPs" were trapped on the sidewall due to magnetic attraction. At the same time, free PMPs that experienced gravitational sedimentation would accumulate in the micro-scale trapping channel with a narrowing nozzle (8 μm in its width). Eventually, the trapping distance of PMP accumulation reflects the concentration of metal ions presented in the sample (Video S3 and Video S4). The channel was connected with a filter paper for capillary pumping. Furthermore, simultaneous loading and reaction with different reagents was demonstrated by integrating three channels in parallel containing different food dye dried in chambers, as shown in Figure 1C.

The workflow of the proposed platform was illustrated in Figure 2A and Figure 2B. To sequentially control the sampling and reaction procedures, the capillary valves were designed at the end of each chamber based on the Young–Laplace equations describing the pressure difference across the interfacial surface of two static phases (i.e., gas and liquid). For example, valve 1 located at the outlet of chamber 1 has a sudden expansion, and the liquid meniscus is trapped at the beginning of the expansion with a specific angle α_2 (Figure 2C). The liquid flowing or stopping at valve 1 depends on the difference between the liquid pressure at outlet P_{1f} and at inlet P_{1e} of the first chamber. (Equation S1-S2). Based on the hydraulic pressure ΔP_{1g} that valve 1 can withstand before bursting (Equation S3-S4), the critical tilting angle β_{1min} of valve 1 can be calculated. The same theory for valve 2 was shown in Equations S5-S8. The criteria for minimal tilting angles of valve 1 (β_{1min}) and valve 2 (β_{2min}) should be $\beta_{2min} > \beta_{1min}$ to ensure that the first tilting will not unintentionally break valve 2, and such difference should be distinguishable by the naked eye to enable the manual operation by unskilled end-users.

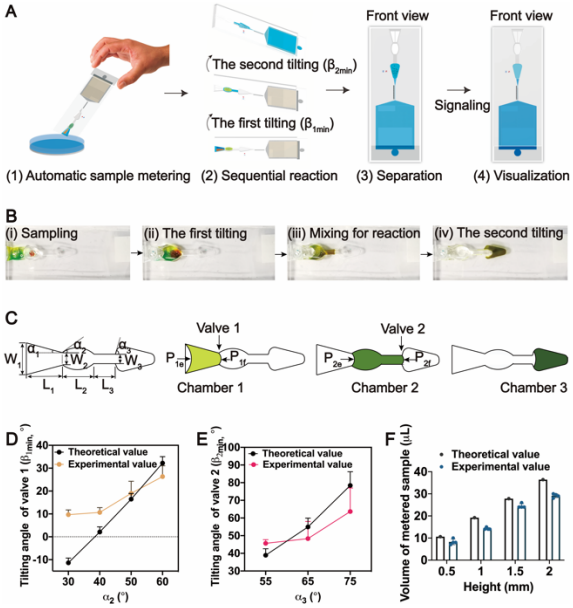

Figure 2. (A) Workflow of the platform. (B) Demonstration of sequential flow by capillary valves using food dye dried in chambers. (C) The sketch diagram of macro-scale chambers. (D) The tilting angle β_{1min} for various expansion angles of valve 1 (α_2). (E) The tilting angle β_{2min} for various expansion angles of valve 2 (α_3). (F) The volume of metered sample for different heights (d) of the first chamber (n = 4).

The expansion angle of valve 1 (α_2) and expansion angle of valve 2 (α_3) were optimized both theoretically and experimentally in advance of obtaining the final design (Figure 2D-2E). With specific widths of valve 1 and valve 2, both the calculated and the measured threshold tilting angles for valve 1 and valve 2 became larger with the increment of expansion angles (α_2 and α_3).

According to the criteria, various dimensions can be obtained with varying lengths, widths, converging angles, and expansion angles (Table S1) for different applications. Finally, the expansion angles α_2 and α_3 were chosen to be 40° and 75°, corresponding to around 9°-13° and 49°-75° of β_{1min} and β_{2min} for the current design. Moreover, valve 1 plays a crucial role in the sample volume metering. Different macro-scale chamber heights (d) were designed to demonstrate that consistent volume sampling can be achieved and is only slightly less than the theoretical value (Figure 2F), meaning that the sampling can be well controlled without the requirement for micro pipetting.

Prior to conduct the assay for metal ions detection, the buffers used for DNAzymes and its corresponding microparticles (MMPs and PMPs) drying were systematically optimized based on the greatest difference of band formation in agarose gel electrophoresis and the PMP trapping distance before and after the presence of metal ion (Figure S2-S4). Finally, 5X PBS buffer (5X PBS, 500 mM NaCl, 0.2% Tween 20) was used for both copper-dependent DNAzyme and its microparticles drying (Figure S2B-C). For Pb^{2+} detection, the Tris-Acetate buffer (50 mM Tris-Acetate, 200 mM NaCl, 0.2% Tween 20) was selected for GR-5 drying and 1X PBS buffer (1X PBS, 500 mM NaCl, 0.2% Tween 20) was used for MMPs and PMPs drying (Figure S3A-B). For Ag^{+} detection, Ag10C DNAzyme and its microparticles were dried in MOPS buffer 1 (50 mM MOPS, 200 mM $NaNO_3$) and MOPS buffer 2 (10 mM MOPS, 40 mM $NaNO_3$, 0.2% Tween 20), respectively (Figure S4A-B). Moreover, the number of PMPs which is closely related to the finally trapping distances has been optimized to be 15×10^3 microspheres (1 µL PMPs in 3% solid) for each assay to obtain the best signal-to-noise ratio (Figure S5). Also, to shorten the turnaround time from sample to results, the hand shaking time for PMPs connections was optimized to be 10 mins (Figure S6). Following the loading of DNAzymes and microparticles and freeze-drying, the detection of Cu^{2+}, $Pb^{2+,}$ and Ag^{+} was first performed separately using the chip with a single channel (Sequences of oligonucleotides can be found in Table S2). For copper ions detection, a series of concentrations of Cu^{2+} (0, 50 nM, 75 nM, 100 nM, 200 nM, 500 nM and 1,000 nM) were applied and the distance of accumulated PMPs was proportional to the concentration of Cu^{2+} (Figure 3A-3C). Using the linear interval from the blank sample (0 - 100 nM), the linear regression equation can be determined as $y = 0.0131x + 0.385 \pm 0.764\sqrt{\frac{1}{3} + \frac{1}{12} + \frac{(x-56.25)^2}{16406.25}}$ (R^2 =0.672), where x represents the concentration of copper ions, and the uncertainties of the intercept s_{b0} and slope s_{b1} are 0.214 and 0.0030 respectively (Supporting Information: Statistical analysis). The LOD was derived to be 103.1 nM, which is around 194 times below the maximum contamination level of 20 µM according to the Environmental Protection Agency in the USA (US EPA). For lead ions detection (Figure 3D-3F), the concentration gradient (0, 50 nM, 75 nM, 100 nM, 200 nM, 300 nM and 500 nM) was managed to obtain the regression equation of $y = 0.0164x + 0.1519 \pm 0.647\sqrt{\frac{1}{3} + \frac{1}{12} + \frac{(x-56.25)^2}{16406.25}}$ (R^2=0.818) by incorporating the uncertainties of the intercept s_{b0} 0.181 and slope s_{b1} 0.0025 respectively. The LOD of 69.5 nM below the toxicity limit of 72 nM defined by the US EPA was achieved using the linear interval from 0 to 100 nM. For silver detection (Figure 3G-3I), on the basis of the linear interval from the blank sample (0 - 1,000 nM), the linear regression equation is $y = 0.0013x + 0.2336 \pm 0.632\sqrt{\frac{1}{3} + \frac{1}{15} + \frac{(x-370)^2}{1914000}}$ (R^2=0.724) with the uncertainties of the intercept s_{b0} 0.124 and slope s_{b1} 0.0002 and the LOD was derived to be 793.6 nM which was lower than the maximum contamination level of 926 nM set by the World Health Organization (WHO). In addition, the selectivity of DNAzyme against other metal ions present in the sample was also explored. More practically, the measurement for each target metal ion with a mixture of other metal ions was also performed, exhibiting high selectivity of 100-fold, 200-fold, and 20-fold for copper, lead, and silver-dependent DNAzymes, respectively (Figure S7).

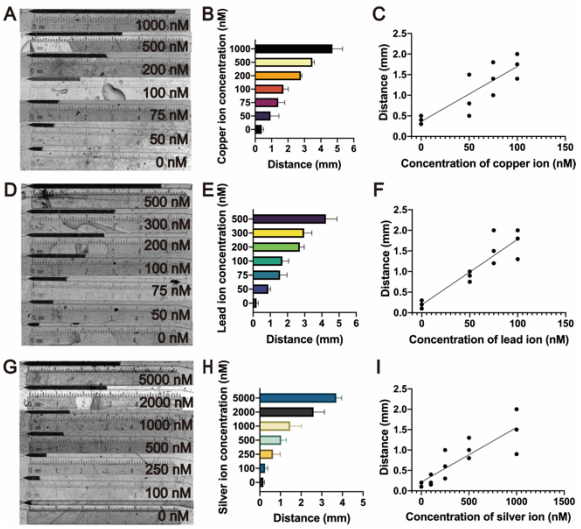

Figure 3. (A-C) Copper ion detection. (A) Optical image of accumulated PMPs (B) The measured distance of accumulated PMPs and (C) Linear regression of PMP accumulation length with respect to Cu^{2+} concentrations. (D-F) Lead ion detection. (D) Optical image of accumulated PMPs (E) The measured distance of accumulated PMPs and (F) Linear regression of PMP accumulation length with respect to Pb^{2+} concentrations. (G-I) Silver ion detection. (G) Optical image of accumulated PMPs (H) The measured distance of accumulated PMPs and (I) Linear regression of PMP accumulation length concerning Ag^{+} concentrations.

Finally, the simultaneous quantification of copper, lead, and silver ions in real samples was conducted by combining three identical channels in parallel (Figure 1C). Freshwater 1 and freshwater 2 were sampled from the *Kowloon reservoir* and *Shek Lei Pui reservoir* (Hong Kong), respectively. Tap water 1 and tap water 2 were sampled from housing buildings at different locations in Hong Kong. As a comparison, samples with spiked metal ions were also examined utilizing the in-house method HOP-EW63 (ICP-OES). To determine the concentrations of target metal ions in real samples,

inverse regression (Supporting Information: Statistical analysis) was applied after reading the trapping distances. The results indicated that the accuracy ranging from 82.9% to 128% was obtained in some cases, demonstrating the practical capability of environmental monitoring. However, lower accuracies that are below 70% were also observed, which partially because of the fluctuation in the interferences amount presented in the real samples.

Overall, the motivation to develop a point-of-care testing device is to allow the platform to be more acceptable and applicable for unskilled end-users. Based on the drying process of micro/nanoparticles as well as fluid dynamics in macro/micro-scale channels, the developed platform integrated sample metering, reaction, and separation with a distance-based display for quantitative measurement which, to a large extent, eliminated the handling barriers, minimized the demanding for fresh preparations of reaction materials and thereby made it more accessible to the general public. Together, it enables wider utilizations as on-site biosensing for environmental, food, and health monitoring for unskilled users in the future.

Table 1. Simultaneous detection of Cu (II), Lead (II) and Silver (I) in fresh water and tap water

Sample	Metal Ions	Spiked (nM)	Found (nM)	ICP-OES (nM)	Accuracy (%)
Fresh water 1	Cu^{2+}	200	155.1 ± 21	173.1	89.5
	Pb^{2+}	200	108.6 ± 24.6	120	90.5
	Ag^{+}	1000	1179.3 ± 193.6	917.8	128
Fresh water 2	Cu^{2+}	200	186.9 ± 30.9	267.5	69.8
	Pb^{2+}	200	120.8 ± 21.4	193	62.6
	Ag^{+}	1000	1204.9 ± 153.8	1112.5	108.3
Tap water 1	Cu^{2+}	100	344.7 ± 27.5	786.9	43.8
	Pb^{2+}	100	57.8 ± 16.1	89.3	64.7
	Ag^{+}	0	63.9 ± 80.1	< 92.7	--
Tap water 2	Cu^{2+}	100	258.1 ± 19.2	401.3	64.3
	Pb^{2+}	100	74.1 ± 7	89.3	82.9
	Ag^{+}	0	25.4 ± 22.2	< 92.7	--

ASSOCIATED CONTENT

Supporting information

The Supporting Information is available free of charge on the ACS Publications website.

Materials and reagents, design and fabrication of chip, design of sequential flow based on Young-Laplace equations, optimization of buffer compositions, on-chip drying of DNAzymes and microparticles, on-chip detection of copper, lead and silver, optimization of the number of PMPs and hand shaking time for particle connection, selectivity and statistical analysis.

Video S1. Sequential flow-Single channel chip (.mp4)

Video S2. Sequential flow-Multichannel chip (.mp4)

Video S3. Particle separation (.mp4)

Video S4. PMPs accumulation (.mp4)

AUTHOR INFORMATION

Corresponding Author

Ting-Hsuan Chen – Department of Biomedical Engineering, City University of Hong Kong, Hong Kong Special Administrative Region, 999077, China; orcid: 0000-0003-4517-7750; Email: thchen@cityu.edu.hk.

Author Contributions

†Gaobo Wang and Jiaheng Li contributed equally to this work.

Notes

The authors declare no competing financial interest.

ACKNOWLEDGMENT

This work was supported by Hong Kong Research Grants Council (11217820 and N_CityU119/19), Innovation and Technology Commission (ITS/098/20) with input from Dr. Iris Wai-Sum Li and Dr. Yinzhong Shen, and The Science, Technology and Innovation Commission of Shenzhen Municipality (JCYJ20210324134006017).

REFERENCES

1. Duruibe, J. O.; Ogwuegbu, M. O. C.; Egwurugwu, J. N. Heavy metal pollution and human biotoxic effects. *Int. J. Phys. Sci.* **2007,** *2* (5), 112-118.

2. Malik, L. A.; Bashir, A.; Qureashi, A.; Pandith, A. H. Detection and removal of heavy metal ions: a review. *Environ. Chem. Lett.* **2019,** *17* (4), 1495-1521.

3. Ferrari, A. G. M.; Carrington, P.; Rowley-Neale, S. J.; Banks, C. E. Recent advances in portable heavy metal electrochemical sensing platforms. *Environ. Sci.: Water Res. Technol.* **2020,** *6* (10), 2676-2690.

4. Liu, L.; Lin, H. W. Paper-Based Colorimetric Array Test Strip for Selective and Semiquantitative Multi-Ion Analysis: Simultaneous Detection of Hg^{2+}, Ag^{+}, and Cu^{2+}. *Anal. Chem.* **2014,** *86* (17), 8829-8834.

5. He, X. C.; Xu, T. L.; Gao, W.; Xu, L. P.; Pan, T. R.; Zhang, X. J. Flexible Superwettable Tapes for On-Site Detection of Heavy Metals. *Anal. Chem.* **2018,** *90* (24), 14105-14110.

6. Hossain, S. M. Z.; Brennan, J. D. β-Galactosidase-Based Colorimetric Paper Sensor for Determination of Heavy Metals. *Anal. Chem.* **2011,** *83* (22), 8772-8778.
7. Muhammad-aree, S.; Teepoo, S. On-site detection of heavy metals in wastewater using a single paper strip integrated with a smartphone. *Anal. Bioanal. Chem.* **2020,** 412 (6), 1395-1405.
8. Lace, A.; Cleary, J. A Review of Microfluidic Detection Strategies for Heavy Metals in Water. *Chemosensors* **2021,** *9* (4), 60.
9. Cate, D. M.; Noblitt, S. D.; Volckens, J.; Henry, C. S. Multiplexed paper analytical device for quantification of metals using distance-based detection. *Lab Chip* **2015,** *15* (13), 2808-2818.
10. Wei, X. F.; Tian, T.; Jia, S. S.; Zhu, Z.; Ma, Y. L.; Sun, J. J.; Lin, Z. Y.; Yang, C. J. Microfluidic Distance Readout Sweet Hydrogel Integrated Paper-Based Analytical Device (μDiSH-PAD) for Visual Quantitative Point-of-Care Testing. *Anal. Chem.* **2016,** *88* (4), 2345-2352.
11. Yamada, K.; Citterio, D.; Henry, C. S. "Dip-and-read" paper-based analytical devices using distance-based detection with color screening. *Lab Chip* **2018,** *18* (10), 1485-1493.
12. Liu, X. L.; Wang, Y. Z.; Song, Y. J. Visually multiplexed quantitation of heavy metal ions in water using volumetric bar-chart chip. *Biosens. Bioelectron.* **2018,** 117, 644-650.
13. Wu, S. Y.; Wu, M. H.; Wang, G. B.; Chen, T. H. Visual quantitation of silver contamination in fresh water via accumulative length of microparticles in capillary-driven microfluidic devices. *Talanta* **2021,** *235,* 122707.
14. Jiang, T. Y.; Wang, G. B.; Chen, T. H. Microfluidic particle accumulation for visual quantitation of copper ions. *Microchim. Acta* **2021,** 188 (5), 176.
15. Wang, G. B.; Chu, L. T.; Hartanto, H.; Utomo, W. B.; Pravasta, R. A.; Chen, T. H. Microfluidic Particle Dam for Visual and Quantitative Detection of Lead Ions. *ACS Sens.* **2020,** *5* (1), 19-23.

For Table of Content Only

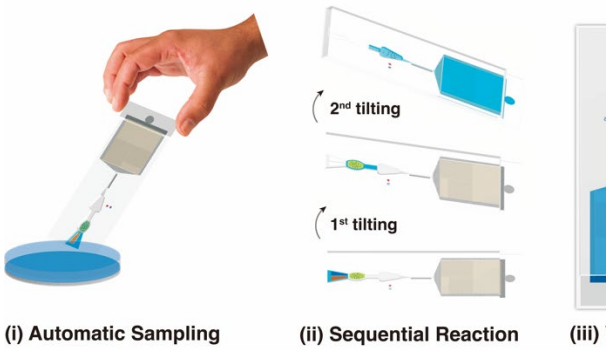

(i) Automatic Sampling (ii) Sequential Reaction (iii)